Food and Bioprocess Technology (2018) 11:2094–2109
https://doi.org/10.1007/s11947-018-2169-3

ORIGINAL PAPER

Radio Frequency-Vacuum Drying of Kiwifruits: Kinetics, Uniformity, and Product Quality

Xu Zhou[1] · Ruzhen Xu[1] · Beihua Zhang[1] · Shaopei Pei[1] · Qianqian Liu[1] · Hosahalli S. Ramaswamy[2] · Shaojin Wang[1,3]

Received: 21 January 2018 / Accepted: 16 August 2018 / Published online: 23 August 2018

Abstract

To overcome long drying time, low energy efficiency and poor product quality associated with conventional drying, a radio frequency (RF) vacuum technology is proposed for drying kiwifruit slices using a 27.12 MHz, 3 kW RF-vacuum drying system. The results demonstrated that the process variables, electrode gap, vacuum pressure, and sample thickness, had major effects on the RF-vacuum drying. The RF-vacuum drying was associated with internal heating and rapid drying resulting in 65% reduction of hot air drying (60 °C) time. Moreover, kiwifruits dehydrated by RF-vacuum drying were associated with better color stability, higher vitamin C retention, and higher rehydration capacity ($p < 0.05$) as compared with hot-air-dried samples. Based on acceptable drying rate, stable temperature and avoiding arcing, a RF-vacuum drying protocol with the electrode gap of 60 mm, vacuum pressure of 0.02 MPa, and sample thickness of 8 mm was identified. Despite some differences observed in individual fruit slices, the RF-vacuum drying technique achieved better and more uniform drying patterns among the samples. Overall, the RF-vacuum drying process may provide a more effective and practical method for high-quality dehydration of kiwifruits.

Keywords Radio frequency-vacuum drying · Hot air drying · Moisture content distribution · Moisture effective diffusivity · Quality

Introduction

Kiwifruit (*Actinidia deliciosa*) is recognized as "the king of fruits" (Huang et al. 2013) due to its remarkably high amounts of vitamin C and bioactive compounds with antioxidant activity. Several studies have demonstrated the beneficial effect of kiwifruits on human health, such as reducing the risk of coronary artery disease and cancer prevention (Bursal and Gulcin 2011; Tavarini et al. 2008). The global production of kiwifruit was around 4.27 million metric tons (Mt) in 2016 mainly contributed by China (2.39 Mt), Italy (0.52 Mt), New Zealand (0.43 Mt), and Chile (0.23 Mt) (FAOSTAT 2018). However, kiwifruit is a seasonal fruit being harvested during August–October in China. Owing to high moisture content, fresh kiwifruit is highly perishable after harvest, even under refrigerated storage conditions (Maskan 2001). Thus, developing a proper postharvest handling technique is an important consideration to overcome the problems of seasonality and extend kiwifruit shelf-life to protect farmers' income and local economy.

Drying is one of the most common preservation technique for improving food storage stability, which reduces the water activity of products below the level that supports the various degradative physiological, biochemical, and microbiological activities in the fruit (Sagar and Kumar 2010; Zhang et al. 2017). In addition, as a result of increase in concentration of various components, drying can offer products with special taste, flavor, and shape. The market for dehydrated vegetables and fruits has been continuously growing worldwide (Zhang et al. 2006). The most conventional drying methods for kiwifruits, such as osmotic dehydration and hot air drying, have low technical barriers in developing/undeveloped countries and are preferred in industry, but with intensive labor cost and high energy consumption (Mujumdar 2007). The long

✉ Shaojin Wang
shaojinwang@nwsuaf.edu.cn

[1] College of Mechanical and Electronic Engineering, Northwest A&F University, Yangling 712100, Shaanxi, China

[2] Department of Food Science and Agricultural Chemistry, McGill University, Montreal H9X 3V9, Canada

[3] Department of Biological Systems Engineering, Washington State University, 213 L.J. Smith Hall, Pullman, WA 99164-6120, USA

drying times along with high temperatures during either hot air drying always result in undesirable quality degradation of final products, including appearance, nutrients, and flavor (Orikasa et al. 2014; Vega-Galvez et al. 2012). Osmotic dehydration is not adequate to reduce moisture contents of food to a desirable level for inhibiting microbial spoilage and therefore used often as a pre-treatment before a secondary drying (Castro-Giraldez et al. 2011; Fathi et al. 2011). In recent years, the popularity of high-quality dehydrated fruit and vegetable has stimulated growing demands for developing novel drying technologies that could provide opportunities to reduce drying time and improve product quality (Zhang et al. 2017).

Microwave (MW) and radio frequency (RF) energy have great potential to overcome the problems of conventional long heating times and prevent product quality degradation due to rapid and volumetric heating (Huang et al. 2018; Ramaswamy and Tang 2008). MW and RF drying methods, also known as dielectric heating, generate heat within the food material by molecular friction as a result of dipolar rotation and ionic conduction (Zhou et al. 2018; Zhou and Wang 2018). There has been extensive research studying the MW and MW-related combination drying for fruits and vegetables, such as mangoes (Pu and Sun 2016, 2017), carrots (Cui et al. 2004; Huang et al. 2016), and blueberries (Zielinska et al. 2015; Zielinska and Michalska 2016). However, MW drying is still limited to small lab-scale investigations (Wang et al. 2014) and difficult to scale up for large industrial implementations because of low penetration depth and non-uniform heating (Ramaswamy and Tang 2008; Zhang et al. 2006).

RF heating has received increasing attention over the past decade due to its longer wavelength and deeper wave penetration as compared with MW and is technologically more feasible for industrial applications (Huang et al. 2018; Marra et al. 2009). RF heating systems have been successfully utilized in food industry, such as baking and roasting (Awuah et al. 2014), cooking (Kirmaci and Singh 2012), disinfesting (Wang et al. 2006; Zhou et al. 2015), pasteurization/sterilization (Jeong et al. 2017; Li et al. 2017; Liu et al. 2018; Zheng et al. 2017), thawing (Bedane et al. 2017; Palazoglu and Miran 2018), and drying (Wang et al. 2014; Zhou et al. 2018a; Zhou and Wang 2018). In general, RF heating is often combined with other conventional drying methods to shorten drying time and improve energy efficiency. For example, a hot air-assisted RF heating was developed to provide a rapid, uniform, and high-quality drying process for in-shell macadamia nuts (Wang et al. 2014) and walnuts (Zhou et al. 2018a). Furthermore, the use of vacuum in RF heating, resulting in RF-vacuum drying (Zhou and Wang 2018), may further raise drying rate and ensure high quality in the final product because of the reduced drying temperatures and oxygen potential as well as considerably higher vapor pressure gradients between the interior and the surface of materials. However, the majority of previous research on this technology has focused on drying of woods (Jia et al. 2015; Koumoutsakos et al. 2001). To the authors' knowledge, there is limited information available in literature about RF-vacuum drying for fruits and vegetables.

Drying uniformity is an important quality parameter in drying technology (Zhang et al. 2017). Wang et al. (2013) used mean moisture content and relative standard deviation of 12 selected processed stem lettuce slices treated with blanching, MW freeze drying, and pulse-spouted MW freeze drying to compare the drying uniformity. Wang et al. (2014) studied weight changes in dried macadamia nuts over 12 compartments in the container to evaluate the drying uniformity of hot air-assisted and RF only treatments. Huang et al. (2016) determined the MW air spouted drying uniformity of carrot cubes in terms of the mass of six randomly selected dehydrated samples and the size of rehydrated samples. More recently, Pu and Sun (2016, 2017) investigated the moisture distribution of a single mango sample during MW-vacuum drying by a hyperspectral imaging technology. Unfortunately, these studies have either just investigated the moisture content difference among the dehydrated samples or focused only on moisture content distribution within the sample. To fully characterize the quality of hot air and RF-vacuum-dried products, it is necessary to evaluate the moisture distribution not only within the individual dried sample but also the sample to sample variability.

Therefore, the objectives of this study were as follows: (1) to determine the effect of RF process variables, such as electrode gap and vacuum pressure, as well as sample thickness on the RF-vacuum drying characteristics of kiwifruit slices; (2) to study the drying kinetics of hot air and RF-vacuum drying as well as determine the effective moisture diffusivity; (3) to evaluate the quality of dried kiwifruit samples in terms of moisture content uniformity, color, vitamin C content, and rehydration capacity.

Materials and Methods

Materials and RF-vacuum Drying System

Freshly harvested kiwifruits (*Actinidia deliciosa* cultivar "Hayward") observed visually for similar ripeness and size (berry radius 51.9 ± 3.5 mm, length 71.5 ± 5.4 mm, weight 131.7 ± 10.2 g) were obtained from Shaanxi, China. After checking carefully to discard blemished kiwifruits, the selected fruits were cold stored in a refrigerator (BCD-220VM, Midea Group Co., Ltd., Foshan, China) at 4 °C. Before testing, the samples were taken out of the cold storage and equilibrated in an incubator (GD/JS4010, Haixiang Instrument & Equipment Co., Ltd., Shanghai, China) at 25 ± 0.5 °C for 12 h. The fruits were then hand peeled and cut into slices with diameter 45.5 ± 5.4 mm and three thicknesses: 6.1 ± 0.2, 8.0 ± 0.2, and 10.0 ± 0.3 mm.

A 3 kW, 27.12 MHz free-running oscillator RF-vacuum drying system (GJ-3-27-JY, Jiyuan High Frequency Electric, Shijiazhuang, China) was used for RF-vacuum drying experiments (Fig. 1). A detailed description of the RF-vacuum system can be found in Zhou et al. (2018b). The RF electrode gaps between the two parallel plates (400 mm × 400 mm) could be adjusted from 20 to 300 mm to deliver desired RF energy for specific applications. The system pressure (vacuum) in the RF chamber and sample temperature and mass were continuously recorded during the entire drying process by a pressure sensor (APC500, Sensor Way Technologies Inc., Beijing, China) located in the vacuum cavity, four-channel fiber-optic sensor system (HQ-FTS-D120, Heqi Technologies Inc., Xian, China), an electronic scale (AT8106, Pengheng Electronic Inc., Shanghai, China) with a precision of 0.1 g mounted underneath the bottom electrode, respectively.

Moisture Content Determination and Drying Procedures

The moisture content of kiwifruit slices was determined following the AOAC Official Method 925.40 (AOAC 2005) and expressed as g [water]/g [solid] through the drying process. For this, about 10–15 g of fruit sample was placed in an aluminum dish and dried at 105 °C under pressure ≤ 13.3 kPa in a vacuum oven until constant weight was achieved. The initial moisture content of fresh kiwifruit slices was 5.66 ± 0.43 kg/kg in dry basis (d.b.).

RF-vacuum drying

Twenty-four freshly prepared kiwifruit slices (523.4 ± 18.0 g) were placed uniformly in a single layer inside a container (400 mm *L* × 270 mm *W* × 20 mm *H*) (Fig. 2a) made of polypropylene (PP) with its side and bottom walls perforated with 10-mm diameter holes. Each sample was separated from the adjacent ones to avoid high-localized temperatures at contact points during RF heating (Hou et al. 2016). The prepared container with kiwifruit slices was placed at the center above the bottom electrode. Three electrode gaps (50, 60, and 70 mm) with three vacuum pressure levels (0.01, 0.02, and 0.03 MPa) and three sample thicknesses (6, 8, and 10 mm) were selected as process/product variables for determining RF-vacuum drying characteristics. These conditions were selected after some preliminary test runs under different conditions to obtain representative RF drying rates and temperatures. The fiber-optic temperature sensors were inserted into the central core of four kiwifruit slices in the geometric center region of the container to record sample temperatures during the RF-vacuum drying process. The sample mass was continuously recorded by the electronic scale without having to turn

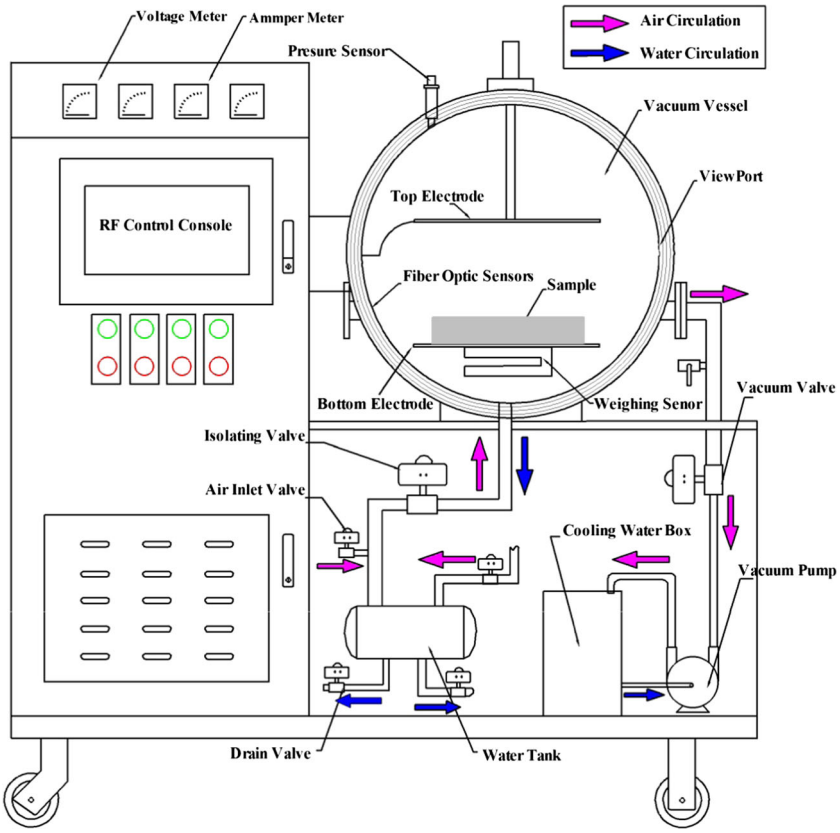

Fig. 1 Schematic view of the 3 kW, 27.12 MHz RF-vacuum drying system showing the plate electrodes, vacuum cavity, and air/water circulations (Zhou et al. 2018b)

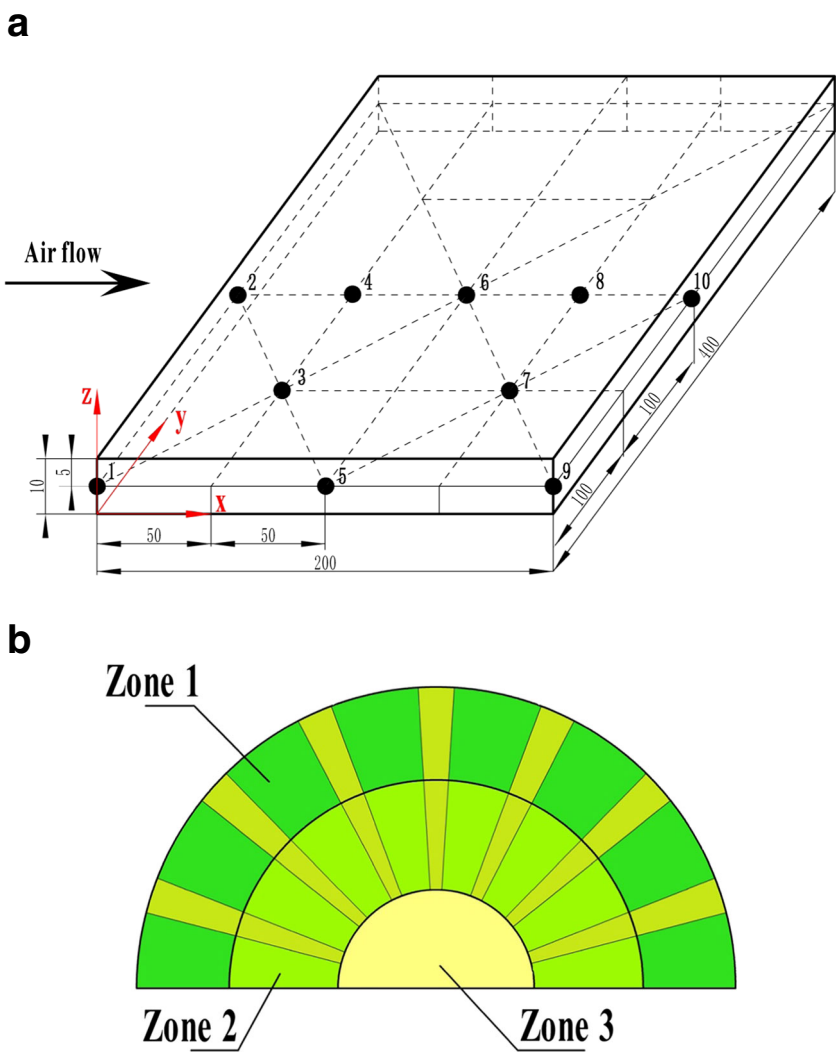

Fig. 2 Rectangular plastic container with 10 compartments (**a**) and three zones (**b**) of the kiwifruit tissue for determining moisture content distribution (all dimensions are in mm)

off RF power or taking out samples. The RF-vacuum drying process was continued until the moisture content of kiwifruit samples reached 0.18 kg/kg (d.b.), which was chosen as the endpoint based on the other studies (Diamante et al. 2010; Orikasa et al. 2014) for hot air drying kiwifruit slices to reach a safe level moisture content (water activity) for long-term storage and without severe product shrinkage or hardening.

Hot air drying

Hot air drying was carried out in a tray dryer (DHG-9030A, Precision & Scientific Instrument Co. Ltd., Shanghai, China) at three temperatures (50, 60, and 70 °C) with an air velocity of 2.0 m/s measured by a rotating vane anemometer (LCA 6000, AIRFLOW Instrumentation, Buckingham-215 Shire, UK). The temperature range and air velocity were selected as being representative of hot air drying of fruits and vegetables (Mrad et al. 2012; Orikasa et al. 2014; Xiao et al. 2010). After startup and achieving steady state conditions in the tray dryer for at least 30 min, 24 kiwifruit slices (thickness 8 mm) were placed in the same type of PP container, and the container was placed on a wire mesh tray mounted at the middle of the convective dryer with a cross flow drying arrangement (Fig. 2a). Every 30 min, the container was taken out of the tray dryer; the surface temperatures of kiwifruit slices and sample mass were quickly measured using a thermal imaging camera (FLIR A300, FLIR Systems AB, Stockholm, Sweden) and an electronic balance with a precision of 0.01 g (PTX-FA210, Huazhi Scientific Instrument, Co., Ltd., Fuzhou, China), respectively. The container was placed back into the convective drying chamber again and drying continued until the moisture content of kiwifruit samples decreased to 0.18 kg/kg (d.b.). The total time interruption for making these measurements was less than 20 s.

Each drying test was repeated thrice. The residual moisture content of kiwifruit samples was calculated based on the initial moisture content and the transient moisture loss during the drying process.

Core and Sub-surface Temperature-Time History

The hot air drying test at 60 °C was selected as a representative of conventional air drying to compare with RF-vacuum drying (electrode gap 60 mm and vacuum pressure 0.02 MPa) in terms of temperature-time history of kiwifruit slices (8 mm) at the sample sub-surface and core. Four fiber-optic sensor probes were inserted into two kiwifruit slices located in the center of the plastic container at about 2.0 mm (sub-surface) and 20.0 mm (core), respectively, which were perpendicular to the kiwifruit slice stem. The temperatures of kiwifruit sample core and sub-surface were recorded at 30 min intervals and used to compare RF and conventional heating characteristics.

Mathematical Modeling of Drying Curves

The macroscopic and microscopic mechanism of moisture diffusion can be described by different drying kinetics (Xiao et al. 2010). Characterization of drying behavior and data on drying models is useful for process design, equipment optimization, and product quality control (Zhang et al. 2017; Zhou and Wang 2018). Table 1 lists six common thin-layer drying models developed for different food products.

The transient changes in moisture content of kiwifruit samples during drying were expressed as moisture ratio (*MR*) defined as:

$$MR = \frac{M_{\mathrm{i}} - M_{\mathrm{e}}}{M_o - M_{\mathrm{e}}} \tag{1}$$

Drying rate (*DR*) was defined as:

$$DR = \frac{M_{\mathrm{i}} - M_{i\text{-}1}}{\Delta t} \tag{2}$$

where *MR* is the dimensionless moisture ratio, M_{i} or $M_{\mathrm{i-1}}$ (kg/kg, d.b.) is the moisture content at any time *i* or *i−1*, Δt is the drying time interval between time *i* and *i−1* (min), which were 15 and 30 min for RF and hot air drying, respectively, in this study, M_0 is the initial moisture content (kg/kg, d.b.) and *Me* is the equilibrium moisture content (kg/kg, d.b.). During the drying period, 20 or 22 of transient drying rates were computed and plotted to draw the RF or hot air drying rate curve. The range of relative humidity (RH) in this drying study was 8–20%, so the M_e ranged from 5–8% and was determined as an average value of 6.5% (kg/kg, d.b.) based on the sorption isotherms of kiwifruits (ASAE 1996; Kaya et al. 2010).

To mathematically describe drying models of food, experimental *MR* data of kiwifruit samples was plotted against *t* and regression analysis was performed with the six thin layer drying models (Table 1). In general, the coefficient of determination (R^2) and root mean square error values (*RMSE*) are the most primary criteria to evaluate the fitness of drying models (Erbay and Icier 2010; Midilli et al. 2002), which were calculated as follows:

$$R^2 = \left(\frac{N\sum_{i=1}^{N} MR_{pre,i} MR_{\exp,i} - \sum_{i=1}^{N} MR_{pre,i} \sum_{i=1}^{N} MR_{\exp,i}}{\sqrt{\left(N\sum_{i=1}^{N} MR_{pre,i}^2 - \left(\sum_{i=1}^{N} MR_{pre,i}\right)^2\right)\left(N\sum_{i=1}^{N} MR_{\exp,i}^2 - \left(\sum_{i=1}^{N} MR_{\exp,i}\right)^2\right)}} \right)^2 \tag{3}$$

$$RMSE = \sqrt{\frac{1}{N}\sum_{i=1}^{N}\left(MR_{pre,i} - MR_{\exp,i}\right)^2} \tag{4}$$

where *N* and *n* are the number of observation and constants, respectively. $MR_{\mathrm{pre,i}}$ and $MR_{\mathrm{exp,i}}$ are the *i*th predicted and experimental *MR* values, respectively.

Calculation of Moisture Effective Diffusivity

Owing to limited knowledge on complex moisture transfer mechanisms during drying, moisture effective diffusivity is generally used as a parameter to determine drying characteristics (Xiao et al. 2010; Erbay and Icier 2010). Given the assumptions of neglecting shrinkage, uniform initial sample moisture content distribution, constant heat, and mass transfer diffusivity, the solution of the Fick's second law of diffusion can be given for various sample geometrics during the falling drying rate period (Crank 1975):

$$MR = \frac{M_{\mathrm{i}} - M_{\mathrm{e}}}{M_o - M_{\mathrm{e}}} = \frac{8}{\pi^2}\sum_{n=0}^{\infty}\frac{1}{(2n+1)^2}\exp\left(\frac{-(2n+1)^2\pi^2 D_{\mathrm{eff}} t}{4(h)^2}\right) \tag{5}$$

where the kiwifruit slice sample considered as the homogeneous slab, D_{eff} is the effective moisture diffusivity (m^2/s), *h* is the half thickness of the slab (*m*), and *n* is a positive integer. For long drying process, Eq. (5) can be simplified in practice when the first term of series solution is applied (Crank 1975):

$$MR = \frac{M_{\mathrm{i}} - M_{\mathrm{e}}}{M_o - M_{\mathrm{e}}} = \frac{8}{\pi^2}\exp\left(\frac{-\pi^2 D_{\mathrm{eff}} t}{4(h)^2}\right) \tag{6}$$

Eq. (6) can then be simplified and expressed in the logarithmic form:

$$\ln(MR) = \ln\left(\frac{8}{\pi^2}\right) - \frac{\pi^2 D_{\mathrm{eff}} t}{4(h)^2} \tag{7}$$

According to Eq. (7), it is clear that the plot of ln (*MR*) versus *t* (min) would be linear, and the slope can be used to calculate the effective moisture diffusion coefficient (D_{eff}).

Table 1 Parameters and performance of six thin-layer drying models for two drying methods

Model	Parameter	Hot air	RF-vacuum
Newton	R^2	0.9915	0.9656
$MR = \exp(-kt)$	*RMSE*	0.0099	0.0691
	k	0.0054	0.0163
Page	R^2	0.9998	0.9803
$MR = \exp(-kt^n)$	*RMSE*	0.0056	0.0321
	k	0.0015	0.0023
	n	1.2014	1.4254
Henderson and Pabis	R^2	0.9892	0.9827
$MR = a\cdot\exp(-kt)$	*RMSE*	0.0271	0.0303
	a	1.1132	1.0421
	k	0.0080	0.0149
Wang and Singh	R^2	0.9790	0.9741
$MR = 1\text{-}at\text{-}bt^2$	*RMSE*	0.0442	0.0572
	a	− 0.0038	− 0.0106
	b	5.0411×10^{-6}	2.4750×10^{-5}
Logarithmic	R^2	0.9951	0.9977
$MR = a\cdot\exp(-kt)+c$	*RMSE*	0.0166	0.0145
	a	1.2113	1.1023
	c	− 0.0851	0.0205
	k	0.0050	0.0128
Midilli	R^2	0.9935	0.9805
$MR = a\cdot\exp(-kt^n) + bt$	*RMSE*	0.0281	0.0452
	a	1.0030	1.0554
	b	6.2649×10^{-4}	7.2214×10^{-5}
	k	0.0409	0.0211
	n	0.9361	0.9985

Evaluation of Product Quality

Moisture Content Uniformity

Moisture content uniformity evaluation involved two aspects: one was moisture distribution among dried kiwifruit slices in the container, and another one was moisture distributions within the fruit slice sample. For the moisture distribution in dried bulk samples, the moisture contents of kiwifruit slices located at 10 representative container locations (#1 to 10; Fig. 2a) were measured after drying. For the moisture distribution of an individual sample, the kiwifruit slice was cut into three zones based on kiwifruit pulp tissue types (Castro-Giraldez et al. 2011) where zones 1, 2, and 3 represented kiwifruit slice outer pericarp, inner pericarp, and core, respectively (Fig. 2b). Four dried kiwifruit slices were taken out from the central part of the container, and each slice was gently cut with a sharp blade into the three zones. The moisture content of each zone was measured by the vacuum oven method (AOAC 2005). The experiments were repeated thrice for each test, and data were used to get estimates of moisture distribution.

Color

The color of fresh (control) and dried kiwifruit slice samples was measured using a computer vision system, which included a lighting system and a Cannon EOS 600 Digital camera with 1800 megapixel resolution and EF-S 18–55 mm f/3.5–5.6 Zoom Lens interfaced to a computer. Detailed information about the color measurement system and procedure can be found in Zhou et al. (2015). The color was expressed in the CIE systems where the values of L^*, a^*, b^* presented darkness-lightness, greenness-redness, and blueness-yellowness, respectively. The total value of color difference (ΔE) was calculated as follows:

$$\Delta E = \sqrt{\left(L^* - L_0^*\right)^2 + \left(a^* - a_0^*\right)^2 + \left(b^* - b_0^*\right)^2} \quad (8)$$

where ΔE is color change, L_0^* and L^* are the lightness values of fresh and dried kiwifruit samples, respectively, a_0^* and a^* are the greenness-redness values of fresh and dried samples, respectively, and b_0^* and b^* are the blueness-yellowness values of fresh and dried samples, respectively. Four dried kiwifruit slices taken out from the center of the container as described above were used for color determination, which was carried out in triplicated samples.

Vitamin C (Ascorbic Acid) Content

Ascorbic acid content was determined by the standard 2,6-dichloroindophenol titration method (Kaya et al. 2010). Ascorbic acid was measured as dehydroascorbic acid following the oxidization of reduced ascorbic acid with the 2,6-dichloroindophenol and expressed as micrograms per gram solids. Four dried kiwifruit slices from each of the triplicate test run described previously were used to determine the ascorbic acid content.

Rehydration Capacity

Rehydration capacity of dried kiwifruit slices was measured according to the method of Maskan (2001) with some modifications. Four dried kiwifruit samples selected from the center of the plastic containers were weighed and then immersed into a beaker containing hot water (50 °C). After 15 min, the kiwifruit slices were removed and drained over a filter paper for 25 s to remove the water adhered to the surface and then reweighed. The rehydration capacity was expressed as percentage of weight gain from the initial weight and calculated as follows:

$$\text{Rehydration capacity} = \frac{W - W_0}{W_0} \times 100\% \quad (9)$$

where W_0 and W are the sample weight values (g) before and after rehydration, respectively.

Statistical Analysis

Test results were expressed as mean ± standard deviations of all observations from the three replicates. Significant difference test was done using Microsoft Excel variance procedure (Microsoft Office Excel, 2010) to determine the difference between the means ($p < 0.05$). The non-linear regression analysis was carried out using statistical analysis software SPSS 16.0 version (SPSS Inc., Chicago, IL, USA) with the coefficient of determination (R^2) and the root mean square error (*RMSE*), which were used to evaluate the fitness of drying models.

Results and Discussions

RF-vacuum Drying Characteristics

Effect of RF Electrode Gap

Figure 3 shows the effect of electrode gap on RF-vacuum heating and drying characteristics of kiwifruit slices. The total drying times required to reduce the moisture content of fruit samples from 5.66 to 0.18 kg/kg (d.b.) were 178, 245, and 320 min for sample thickness 8 mm and vacuum pressure 0.02 MPa, at electrode gaps of 50, 60, and 70 mm, respectively (Fig. 3a). The heating rates decreased with increasing electrode gap due to decreasing electric field intensity (Fig. 3b). The average sample temperatures at the different electrode gaps also increased gradually to their highest value during the RF heating and then remained relatively constant near the saturation temperature of water under the vacuum pressure of 0.02 MPa until the moisture content reached about 0.50 kg/kg (d.b.) (Fig. 3d). While the sample temperature remained steady, the drying rate increased rapidly and reached the peak because the absorbed RF energy was mostly used for moisture evaporation. Surface diffusion would be the dominant mechanism governing the mass transfer at this stage (constant drying rate period). Generally, the smaller electrode gap resulted in higher RF heating—drying rates, but also resulted in some non-uniform heating and sometimes runaway heating occurred at the corners and edges of the products as has been observed in other studies (Huang et al. 2015; Marra et al. 2009; Tiwari et al. 2011). To obtain both relatively rapid drying rate and acceptable heating uniformity, the electrode gap of 60 mm was selected for drying kiwifruit slices in the subsequent tests.

Effect of Vacuum Pressure

Figure 4 shows the effect of different vacuum pressures (0.01, 0.02, and 0.03 MPa) on RF-vacuum heating—drying characteristics with 60 mm electrode gap and 8 mm sample thickness, suggesting that RF-vacuum drying time decreased at lower vacuum pressure levels (higher vacuum). For example, the RF-vacuum drying time at the vacuum pressure of 0.03 MPa was 330 min, and it decreased approximately 40% when the vacuum pressure applied was 0.01 MPa (Fig. 4a). The moisture diffusion rate was elevated by lowering the vacuum pressure due to the increased vapor pressure gradients. Similar results have also been reported for MW-vacuum drying of fruits/vegetables, such as carrot slices (Cui et al. 2004), apple slices (Han et al. 2010), and edamames (Hu et al. 2006). However, too low vacuum pressure during MW/RF drying may cause some potential technical problems, including dielectric breakdown (arcing) and glow discharges, leading to local overheating and possible scorching of final products (Zhang et al. 2006). Therefore, a moderate vacuum pressure level of 0.02 MPa was selected for the further drying tests to avoid possible arcing phenomenon and reduce vacuum operating costs.

Effect of Sample Thickness

The influences of kiwifruit slice thickness on RF-vacuum drying characteristics were somewhat lower than those of electrode gap and vacuum pressure (Fig. 5). When the sample thickness increased from 6 to 10 mm, the RF-vacuum drying time only increased by 16% at the tested

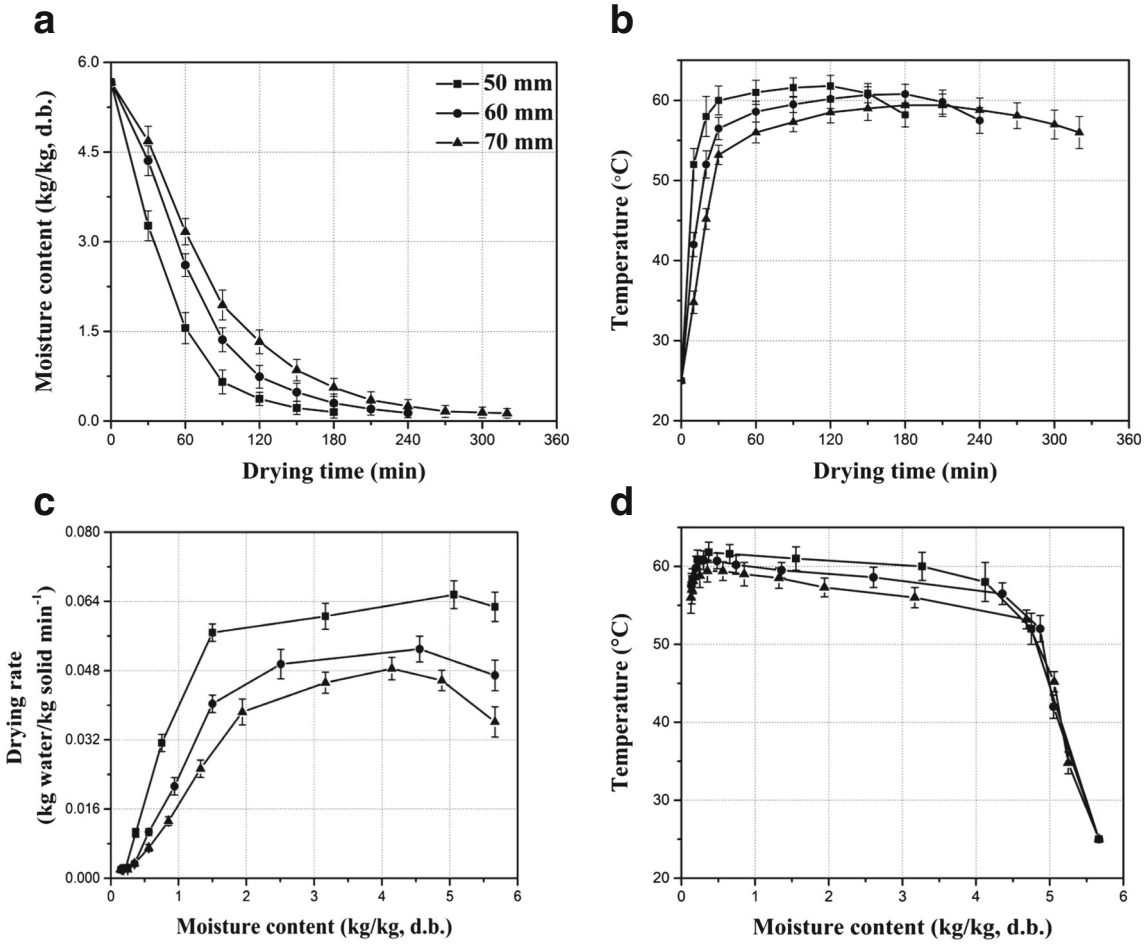

Fig. 3 Changes in sample moisture contents (**a**), temperatures-time history (**b**), drying rates (**c**), and temperature-moisture content history (**d**) with electrode gaps of 50, 60, and 70 mm under constant vacuum pressure (0.02 MPa) and sample thickness (8 mm) during RF-vacuum drying

electrode gap and vacuum pressure levels (60 mm gap and 0.02 MPa vacuum pressure) (Fig. 5a). Although the moisture diffusion path from the interior to the surface increases with an increasing sample thickness (Villa-Corrales et al. 2010), heat is generated within materials by polar molecular friction during RF drying and as a result positive internal thermal and pressure gradients enable efficient moisture vaporization and expulsion toward the surface. However, this phenomenon was different from that observed in convective and microwave drying. For example, the hot air drying time was reported to increase by about 40% when yam slice thickness increased from 5 to 7 mm (Ju et al. 2016). The MW-vacuum drying time for kiwifruit slices was also reported to increase from 9 to 20 min when sample thickness increased from 4 to 12 mm (Tian et al. 2012). Although MW and RF have similar heating mechanisms, the smaller penetration depth associated with MW as compared with RF heating is likely responsible for the slower heating rate associated with the former. In this study, the RF heating rate of kiwifruit slices even increased with increasing sample thickness (Fig. 5b). This was because the air gap between top electrode and upper surface of sample simultaneously decreased with the increasing sample thickness, resulting in more intense RF electric field distribution and faster heating rate (Tiwari et al. 2011; Uyar et al. 2014). Therefore, RF drying offers better advantages of heating/drying larger size or bulk materials as compared with MW and convective drying. Since increasing sample thickness leads to an increasing moisture diffusion path and reducing the gap between the sample and electrode, a sample thickness of 8 mm was selected for the further evaluation of RF-vacuum drying process.

In general, the RF-vacuum drying profile involved three stages regardless of various operating parameters. Stage I in which RF energy was transformed into thermal one within the materials and sample temperature rapidly increased. Once the moisture vapor pressure in the samples exceeded that of environment, the moisture expulsion process got, and the drying rate gradually increased. Stage II began when the product temperature reached the highest value (wet bulb temperature), the drying process entered into a rapid drying period (constant drying rate period), and the sample temperature remained at a

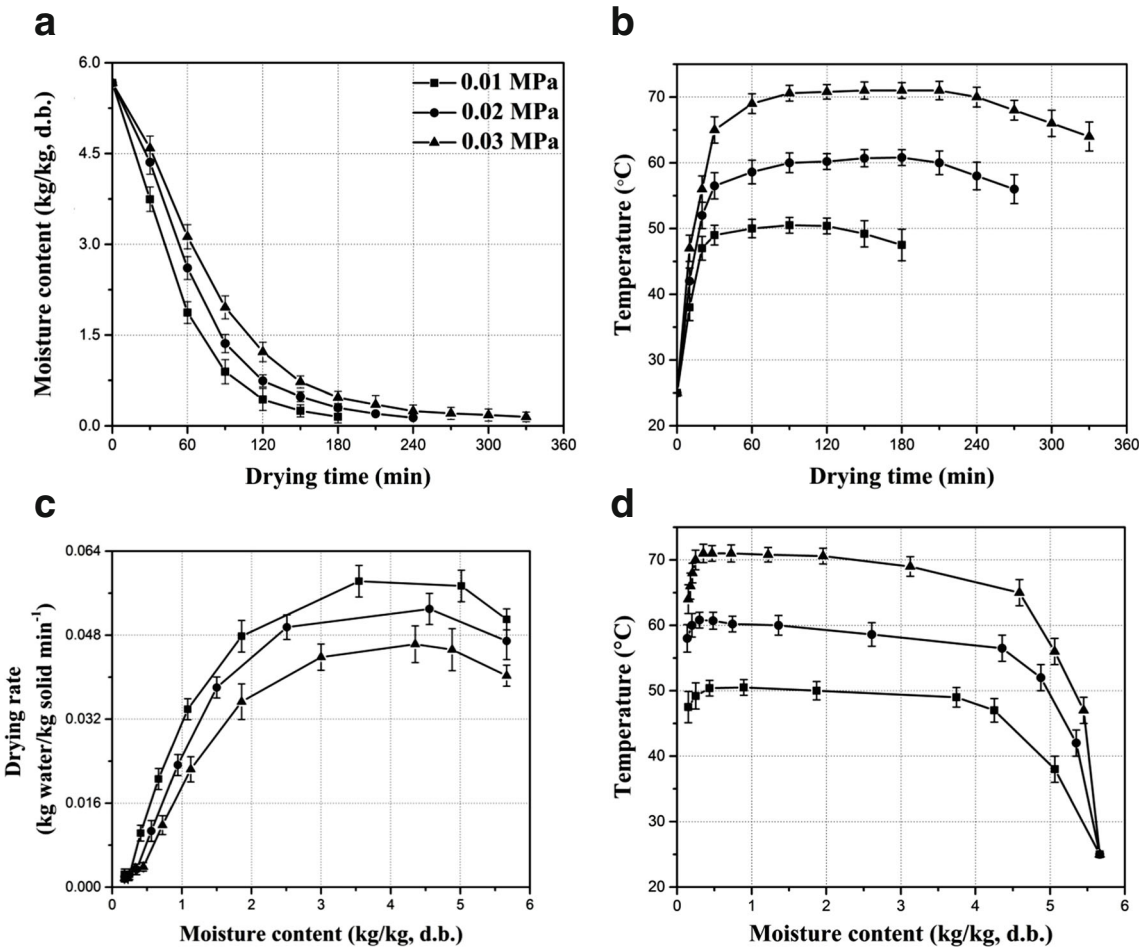

Fig. 4 Changes in sample moisture contents (**a**), temperatures-time history (**b**), drying rates (**c**), and temperature-moisture content history (**d**) with vacuum pressures of 0.01, 0.02, and 0.03 MPa under constant electrode gap (60 mm) and sample thickness (8 mm) during RF-vacuum drying

fairly constant level. As the drying progressed into Stage III, the loss of water in the samples reduced the associated dielectric properties, resulting in reduced absorption of RF energy, and led to a gradually decreasing rate of drying toward the final stage of drying (Zhou and Wang 2018) (Figs. 3d, 4d, and 5d). Additionally, the thermal energy required for breaking away bound water is higher than that required for free water (Therdthai and Zhou 2009). Consequently, the RF-vacuum drying rate gradually decreased, and the drying process was dominated by the falling drying rate period (Stage III). These trends were also similar to those reported in hot air-assisted RF drying for in-shell nuts (Wang et al. 2014; Zhou et al. 2018a). However, in most case of MW-vacuum drying, especially at the final stage, localized sample temperatures rise above the boiling point of water (Cui et al. 2004; Huang et al. 2016). Even with reduced loss factor of dielectric materials due to moisture reduction, sample temperature would continue to increase, resulting in thermal runaway or charring (Zhang et al. 2006). In other words, the RF-vacuum drying process may limit the temperature raise in the samples and reduce severe thermal deterioration of product quality.

Hot Air Drying Characteristics

Figure 6 shows that hot air drying at 50, 60, and 70 °C required 700, 540, and 330 min, respectively, for reducing the initial moisture content of kiwifruit samples to the final level (0.18 kg/kg, d.b.). The sample average surface temperature increased gradually with drying time but was always below the hot air set points (Fig. 6b). In addition, the heating rate decreased steadily with drying time. Generally, the drying time decreased significantly with increasing air temperatures, which is in agreement with previous studies about convective drying for fruits and vegetables, such as grapes (Xiao et al. 2010), apples (Vega-Galvez et al. 2012), and yams (Ju et al. 2016). Moreover, the drying rate decreased continuously as the moisture content decreased and in fact the hot air drying only occurred in the falling rate period at all temperatures studied (Fig. 6c). The absence of constant drying rate period was because the liquid or vapor diffusion was the dominant mass transfer mechanism of fruits during the hot air drying process (Simal et al. 2005; Xiao et al. 2010).

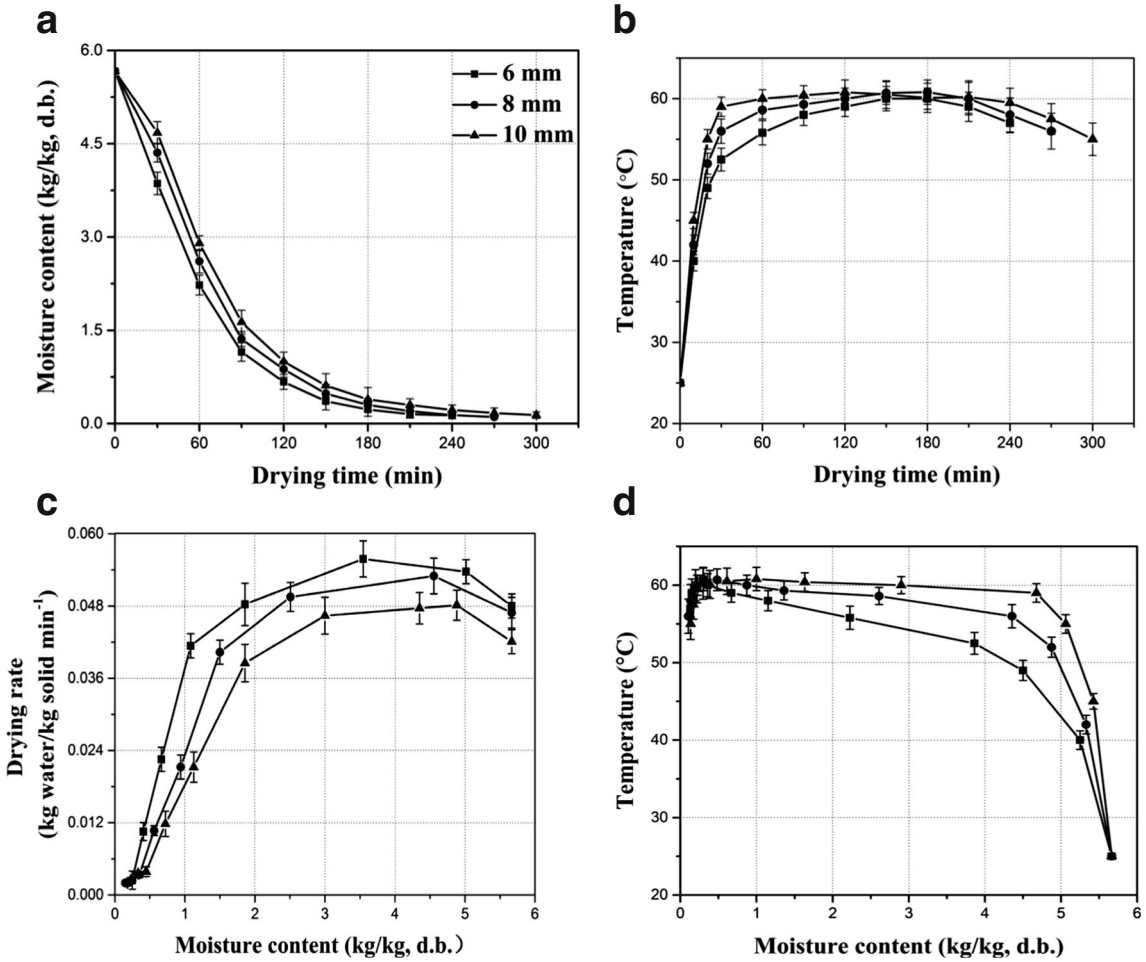

Fig. 5 Changes in sample moisture contents (**a**), temperatures-time history (**b**), drying rates (**c**), and temperature-moisture content history (**d**) with sample thicknesses of 6, 8, and 10 mm under constant electrode gap (60 mm) and vacuum pressure (0.02 MPa) during RF-vacuum drying

Core and Sub-surface Temperature-Time History

Figure 7 shows a typical drying temperature-time profile at the core and sub-surface of kiwifruit slices subjected to RF-vacuum and hot air drying, indicating that the RF-vacuum-dried materials were heated throughout the sample whereas surface higher temperatures were found in hot air drying. Particularly, the RF heating rate was much higher than that of hot air drying at both sample core and sub-surface, especially in the initial stage of drying. The average sub-surface temperature of samples increased immediately when subjected to RF-vacuum drying, but it started to increase after about 5–8 min in hot air drying. For hot air drying, it took 660 min to raise the core temperature of kiwifruit slice sample to reach 58 °C while only 90 min was required for RF-vacuum drying heated samples to reach 60 °C. Moreover, the heating patterns for sample core were similar to those for sub-surface during the RF-vacuum drying due to the volumetric heating characteristics. The internal RF heating pattern was similar to the results observed in other studies with apple (Wang et al. 2006), orange (Birla et al. 2008), and almond (Jeong et al. 2017). In contrast, the different temperature distribution that was observed from the surface to the center of kiwifruit slices during the hot air drying was due to the high external and internal heat transfer resistance across the samples (Esfahani et al. 2014). As hot air drying progressed, the temperature gradient between core and sub-surface of kiwifruit slices gradually decreased. This may be because the heating rate of wet core decreased more rapidly by evaporating more water than in the dry surface. In addition, the heat gain by convective transfer was balanced by the heat transfer through conduction (Esfahani et al. 2014).

Drying Kinetics and Moisture Effective Diffusivity

Table 1 summarizes the regression and correlation analyzes of hot air drying (60 °C) and RF-vacuum drying (electrode gap of 60 mm and vacuum pressure of 0.02 MPa) of kiwifruit slices (8 mm) with six drying kinetic models. The results show that the Page model (R^2 of 0.9998 and *RMSE* of 0.0056) was the best fit to describe hot air drying while the logarithmic model (R^2 of 0.9977 and *RMSE* of 0.0145) provided the best fit for RF-vacuum drying. On the other hand, Wang and Singh

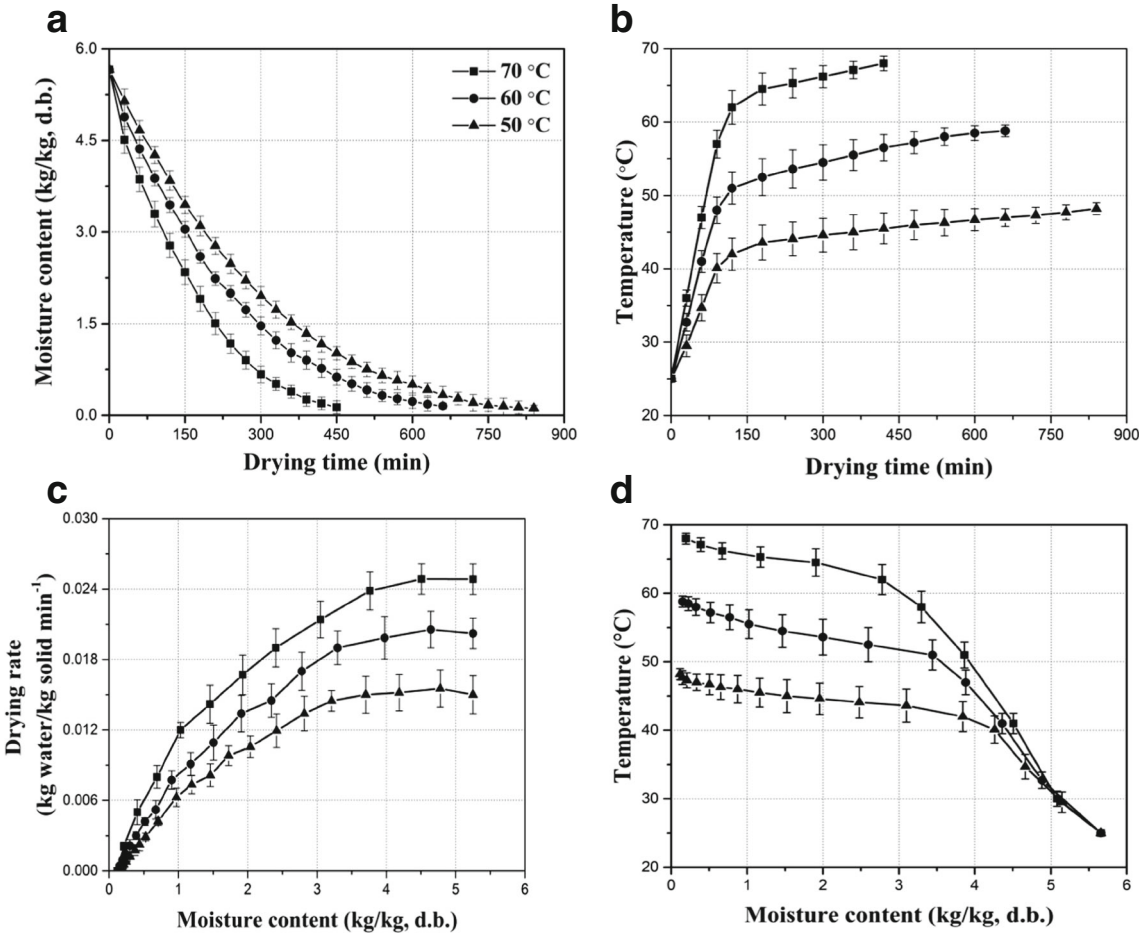

Fig. 6 Changes in sample moisture contents (**a**), surface temperatures-time history (**b**), drying rates (**c**), and temperature-moisture content history (**d**) at different drying temperatures (50, 60, and 70 °C) under constant air velocity (2.0 m/s) and sample thickness (8 mm) during hot air drying

model resulted in the worst fit for both hot air and RF-vacuum drying with R^2 of 0.9790 and 0.9741, respectively. The drying constant k of RF-vacuum drying was higher than that of hot air drying in Page model, indicating better drying rates with the RF-vacuum. This result further confirmed the earlier observation that RF-vacuum drying improved kiwifruit's drying performance. Additionally, the identified parameter n of hot air drying was higher than the value obtained in other studies (Simal et al. 2005), probably due to the higher sample thickness (8 mm) as compared to the previous study (6 mm). Parameter a in the logarithmic model can be regarded as a critical MR, distinguishing the two different drying rate periods (Erbay and Icier 2010). This is in good agreement with studies reported by Orikasa et al. (2014) and Simal et al. (2005). The curves for MR versus drying time with the best drying models under hot air and RF-vacuum drying are shown in Fig. 8. Generally, the drying time for kiwifruit slices was reduced by about 65% when using RF-vacuum drying technology as compared to hot air drying, highlighting the advantage associated with RF-vacuum drying technology.

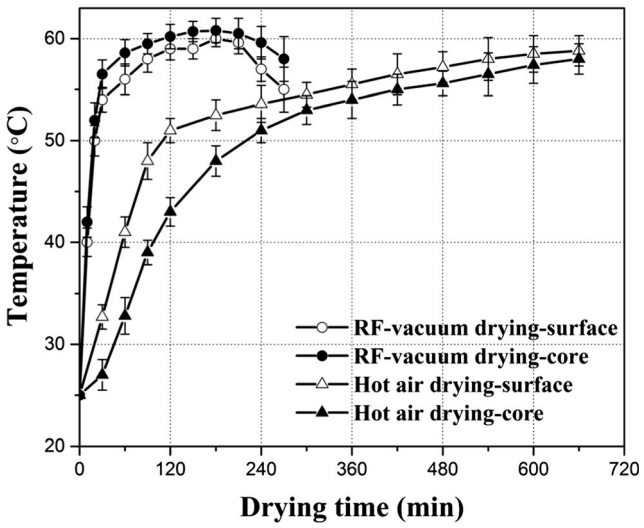

Fig. 7 Typical temperature-time history for sub-surface (2 mm) and core (20 mm) of kiwifruit slices (8 mm thickness and 45 mm diameter) when subjected to hot air (60 °C) and RF-vacuum drying (electrode gap of 60 mm and vacuum pressure of 0.02 MPa)

The moisture effective diffusivity (D_{eff}) value is another parameter that is associated directly with the drying rate. D_{eff} values for hot air and RF-vacuum drying were 10.18×10^{-10} and 18.92×10^{-10} m^2/s, respectively, indicating nearly twice

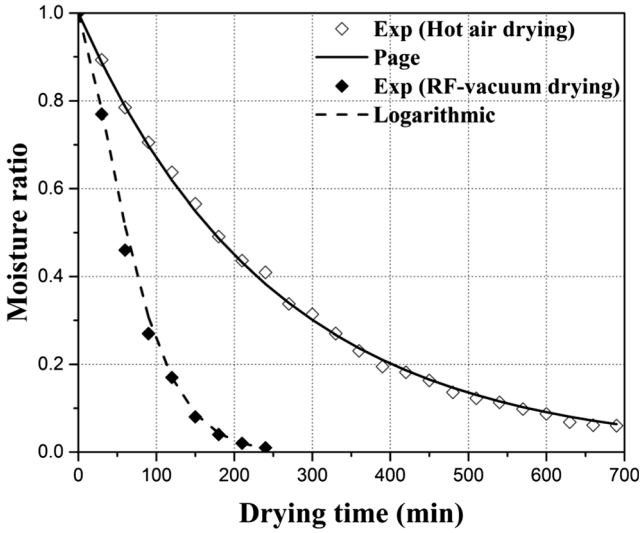

Fig. 8 Drying kinetics of kiwifruit slices when subjected to hot air (60 °C) and RF-vacuum (electrode gap of 60 mm and vacuum pressure of 0.02 MPa) drying fitted with the Page and Logarithmic models against experimental values (Exp)

the diffusivity value with RF-vacuum drying. The estimated D_{eff} values were in the same range reported elsewhere (Erbay and Icier 2010; Simal et al. 2005). Large internal thermal energy input produced by RF heating is the reason for the higher moisture diffusivity values.

Quality of Dried Kiwifruit Slices

Table 2 summarizes the results for kiwifruit product quality after hot air and RF-vacuum drying. The associated higher L^* value as well as lower a^* value and b^* value with RF-vacuum-dried kiwifruits ($p < 0.05$) suggests that the fruit slices treated by hot air were more dark, red, and yellow in color than RF-vacuum-dried ones. The color change of kiwifruits is associated with enzymatic browning or Maillard reaction, depending on drying temperature, time, and oxygen level (Therdthai and Zhou 2009; Vega-Galvez et al. 2012). In general, the total color change (ΔE) of RF-vacuum-dried kiwifruits was significantly smaller ($p < 0.05$) possibly due to the shorter drying time, lower temperatures, and reduced oxygen concentration. Comparing with the control (fresh kiwifruits), however, hot air and RF-vacuum drying demonstrated significant color degradation ($p < 0.05$). For example, mean L^* values decreased with drying time for both dried kiwifruit samples, firstly due to chlorophyll degradation and subsequently as the moisture content decreased due to browning reactions. Therefore, future research is necessary to develop an effective pre-treatment before RF-vacuum drying, such as blanching, dipping, or osmotic dehydration, to avoid color deterioration of final products.

Differences ($p < 0.05$) in the vitamin C content retention were also observed in dried kiwifruits (Table 2). The retention ratio of vitamin C was less than 60% or lower (54% and 40% for RF-vacuum and hot air dehydrated samples, respectively). This phenomenon is caused by the fact that vitamin C is oxygen and heat sensitive and can be degraded through oxidation even under low-oxygen conditions during drying (Kaya et al. 2010; Xiao et al. 2010). The vitamin C content of RF-vacuum-dried kiwifruits was significantly higher ($p < 0.05$) than that of hot-air-dried samples, which was probably due to low concentration of oxygen and short drying time associated with the RF-vacuum drying.

The rehydration capacity of RF-vacuum-dried kiwifruits was significantly higher ($p < 0.05$) than that in hot-air-dried samples (Table 2). During RF-vacuum drying, the positive vapor pressure pushed from within foods leads to the creation of a porous, loose, and fragile texture for the kiwifruits and therefore results in better water absorption capacity. This desirable rehydration capacity has also observed in MW-vacuum-dried products, such as mint leaves (Therdthai and Zhou 2009), beetroots (Figiel 2010), and blueberries (Zielinska and Michalska 2016).

Figure 9 shows the measured moisture distribution in the samples spread over 10 different compartments after the RF-vacuum and hot air drying. For hot air drying, the sample moisture removal was in line with the direction of air flow and resulted in reduced moisture loss as the tray numbers increased from 1 to 10. Hot air was fresh and dry when it hit tray 1 and picked up moisture as it moved forward diminishing its moisture removal potential. Similar results have been observed by Esfahani et al. (2014). Sharp edges and samples in the front areas may cause a wake in the hot air flow and lower the contact potential with the samples in behind faces. On the other hand, the moisture contents of RF-vacuum dehydrated samples were more random and uniform.

Table 2 Quality characteristics (means ± SD over three replicates) of kiwifruit samples before and after drying treatments

	L^*	a^*	b^*	ΔE	Vc content (mg/100 g)	Rehydration capacity (%)
Fresh (control)	42.28 ± 1.01a[#]	− 8.93 ± 0.14c	24.77 ± 0.48a	–	115.35 ± 6.57a	–
Hot air drying	29.75 ± 3.94c	− 0.82 ± 0.81a	20.46 ± 0.61c	15.56 ± 1.41a	45.87 ± 5.68c	115.85 ± 4.59b
RF-vacuum drying	36.46 ± 2.25b	− 5.43 ± 0.49b	22.26 ± 0.46b	7.11 ± 0.86b	62.54 ± 4.77b	148.46 ± 6.84a

[#] Different lower case letters indicate that means are significantly different at $p = 0.05$ among drying methods

Vc vitamin C

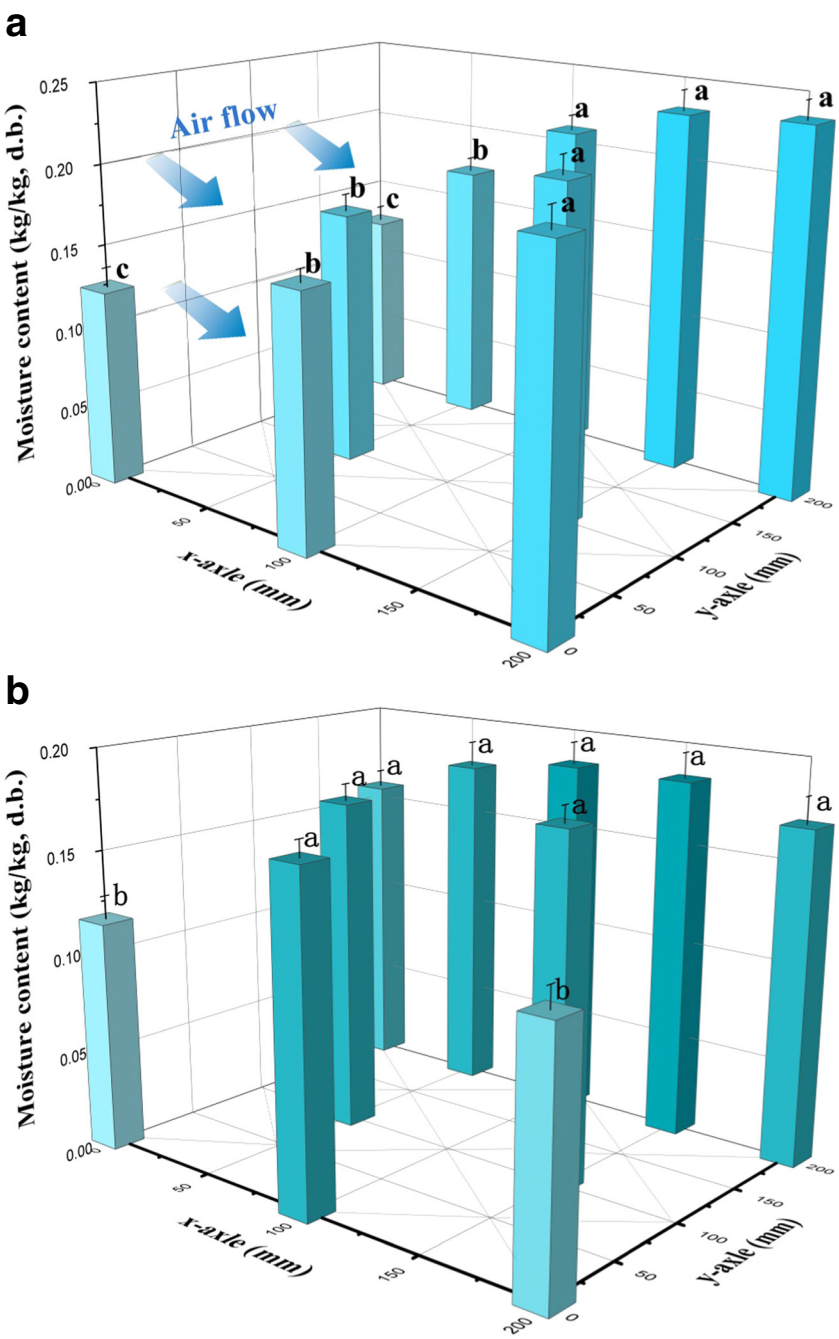

Fig. 9 Moisture content of hot air (**a**) and RF-vacuum (**b**) dried kiwifruit samples at 10 compartments in the container with x-axis parallel to the hot air flow (Fig. 2) (different lower case letters indicate that means are significantly different at $p = 0.05$ among compartments)

They were only slightly higher in trays 3–8 than in 1, 2, 9, and 10. This may be because the RF electric field strength is higher at the edge and corner of the rectangular container than that at center part (Huang et al. 2018; Huang et al. 2015; Tiwari et al. 2011). Based on statistical analysis, no significant difference ($p < 0.05$) was found in moisture contents among the compartments except for 1 and 9, thereby demonstrating relatively more uniform moisture distribution in kiwifruit slices with RF-vacuum drying.

The internal moisture content at three zone locations in fresh and dehydrated kiwifruit slice is shown in Table 3. Lower moisture contents were associated with the center than at pericarp in RF-vacuum dehydrated kiwifruits, which may be because the dissipated energy provided by RF electric field was generated within samples, leading to higher temperature profile and higher moisture diffusion rate in the center. In contrast, the moisture content of hot-air-dried samples increased progressively from the periphery to the core. This is because hot air drying relies on surface heating with convection, and the progressive loss of water causes drying of the surface and shrinkage, which forms a barrier for the further heat transfer and limits moisture diffusion. Case hardening as reported in several studies with air drying results from such thermal barriers with more intensive drying at the food surface (Zhang et al. 2006). In

Table 3 Moisture content (means ± SD over three replicates, d.b.) of three tissue zones (Fig. 2b) of kiwifruit slices before and after drying treatments

	Fresh (control)	Hot air drying	RF-vacuum drying
Whole sample	5.66 ± 0.19aA*	0.19 ± 0.05bB	0.17 ± 0.02bB
Zone 1	5.84 ± 0.26aA	0.08 ± 0.02cC	0.23 ± 0.02aB
Zone 2	5.43 ± 0.24aA	0.16 ± 0.04bB	0.15 ± 0.02bB
Zone 3	4.03 ± 0.32bA	0.32 ± 0.05aB	0.10 ± 0.01cC

* Different lower and upper case letters indicate that means are significantly different at $p = 0.05$ among zones and drying treatments, respectively

general, the moisture distributions within kiwifruit slices corresponded to the temperature-time history at sample core and sub-surface during drying as noted previously. These results are in agreement with Pu and Sun (2016, 2017) who evaluated MW-vacuum drying with mango samples.

Conclusion

The process parameters, electrode gap, and vacuum pressure as well as sample thickness, had major effects on the RF-vacuum drying characteristics of kiwifruits. The suggested drying protocol of RF-vacuum of kiwifruits is electrode gap of 60 mm, vacuum pressure of 0.02 MPa, and kiwifruit slice thickness of 8 mm. As compared to hot air drying (60 °C), the total drying time required to reduce the moisture content of kiwifruit samples from 5.66 kg/kg (d.b.) to 0.48 kg/kg (d.b.) was reduced by more than 65% (690 min to 240 min) by applying the RF-vacuum drying method. Further, the RF-vacuum drying process ensured better quality retention in the dehydrated kiwifruit slices in terms of color, vitamin C content, and rehydration capacity due to fast heating/drying rates and low vacuum pressure. Better uniform moisture distribution was achieved when subjected to the RF-vacuum drying than possible with hot air drying. Overall, RF-vacuum drying technology may provide a more effective and practical dehydration method for kiwifruits with acceptable quality attributes. However, both hot air and RF-vacuum drying may result in a somewhat non-uniform moisture distribution within the fruit slices, and some equilibration technique should be explored to prevent incomplete moisture loss and instability during storage (moisture sorption isotherm studies). Further, future research should explore other combinatorial techniques to take advantage of rapid drying rates and improving quality retention.

Acknowledgements This research was conducted in the College of Mechanical and Electronic Engineering, Northwest A&F University. The authors thank the technical assistance from Shuming Zhang, Rui Li, Shuang Zhang, Lihui Zhang, and Biying Lin for carrying out the experiments.

Funding Information This research was supported by research grants from National Key Research and Development Program of China (2017YFD0400900, 2016YFD0401000), National Natural Science Foundation in China (No. 31772031), and Key Laboratory of Post-Harvest handling of fruits, Ministry of Agriculture (GPCH201703).

References

AOAC. (2005). *Official methods of analysis of AOAC international*. Maryland: Gaithersburg.

ASAE. (1996). *Moisture relationships of plants-based agricultural products. ASAE standards D245.5 OCT95. Agricultural engineering yearbook* (43th ed.pp. 452–464). St. Joseph: ASAE.

Awuah, G., Koral, T., & Guan, D. (2014). Radio-frequency baking and roasting of food products. In B. A. George, H. S. Ramaswamy, & J. Tang (Eds.), *Radio frequency heating in food processing: principles and applications* (pp. 231–243). Boca Raton: CRC Press.

Bedane, T. F., Chen, L., Marra, F., & Wang, S. (2017). Experimental study of radio frequency (RF) thawing of foods with movement on conveyor belt. *Journal of Food Engineering, 201*, 17–25.

Birla, S. L., Wang, S., Tang, J., & Tiwari, G. (2008). Characterization of radio frequency heating of fresh fruits influenced by dielectric properties. *Journal of Food Engineering, 89*(4), 390–398.

Bursal, E., & Gulcin, I. (2011). Polyphenol contents and in vitro antioxidant activities of lyophilised aqueous extract of kiwifruit (*Actinidia deliciosa*). *Food Research International, 44*(5), 1482–1489.

Castro-Giraldez, M., Tylewicz, U., Fito, P. J., Dalla Rosa, M., & Fito, P. (2011). Analysis of chemical and structural changes in kiwifruit (*Actinidia deliciosa* cv *Hayward*) through the osmotic dehydration. *Journal of Food Engineering, 105*(4), 599–608.

Crank, J. (1975). *The mathematics of diffusion* (2nd ed.). London: Oxford University Press.

Cui, Z. W., Xu, S. Y., & Sun, D. W. (2004). Microwave-vacuum drying kinetics of carrot slices. *Journal of Food Engineering, 65*(2), 157–164.

Diamante, L., Durand, M., Savage, G., & Vanhanen, L. (2010). Effect of temperature on the drying characteristics, colour and ascorbic acid content of green and gold kiwifruits. *International Food Research Journal, 17*, 441–451.

Erbay, Z., & Icier, F. (2010). A review of thin layer drying of foods: theory, modeling, and experimental results. *Critical Reviews in Food Science and Nutrition, 50*(5), 441–464.

Esfahani, J. A., Majdi, H., & Barati, E. (2014). Analytical two-dimensional analysis of the transport phenomena occurring during convective drying: apple slices. *Journal of Food Engineering, 123*, 87–93.

FAOSTAT. Food and Agriculture Organization of the United States (2018). http://www.fao.org/faostat/en/#data. Access date: January, 2018.

Fathi, M., Mohebbi, M., & Razavi, S. M. A. (2011). Application of image analysis and artificial neural network to predict mass transfer kinetics and color changes of osmotically dehydrated kiwifruit. *Food and Bioprocess Technology, 4*(8), 1357–1366.

Figiel, A. (2010). Drying kinetics and quality of beetroots dehydrated by combination of convective and vacuum-microwave methods. *Journal of Food Engineering, 98*(4), 461–470.

Han, Q. H., Yin, L. J., Li, S. J., Yang, B. N., & Ma, J. W. (2010). Optimization of process parameters for microwave vacuum drying of apple slices using response surface method. *Drying Technology, 28*(4), 523–532.

Hou, L., Huang, Z., Kou, X., & Wang, S. (2016). Computer simulation model development and validation of radio frequency heating for bulk chestnuts based on single particle approach. *Food and Bioproducts Processing, 100*, 372–381.

Hu, Q. G., Zhang, M., Mujumdar, A. S., Xiao, G. N., & Sun, J. C. (2006). Drying of edamames by hot air and vacuum microwave combination. *Journal of Food Engineering, 77*(4), 977–982.

Huang, S. X., Ding, J., Deng, D. J., Tang, W., Sun, H. H., Liu, D. Y., Zhang, L., Niu, X. L., Zhang, X., Meng, M., Yu, J. D., Liu, J., Han, Y., Shi, W., Zhang, D. F., Cao, S. Q., Wei, Z. J., Cui, Y. L., Xia, Y. H., Zeng, H. P., Bao, K., Lin, L., Min, Y., Zhang, H., Miao, M., Tang, X. F., Zhu, Y. Y., Sui, Y., Li, G. W., Sun, H. J., Yue, J. Y., Sun, J. Q., Liu, F. F., Zhou, L. Q., Lei, L., Zheng, X. Q., Liu, M., Huang, L., Song, J., Xu, C. H., Li, J. W., Ye, K. Y., Zhong, S. L., Lu, B. R., He, G. H., Xiao, F. M., Wang, H. L., Zheng, H. K., Fei, Z. J., & Liu, Y. S. (2013). Draft genome of the kiwifruit Actinidia chinensis. *Nature Communications, 4*(1), 2640.

Huang, Z., Zhu, H., Yan, R., & Wang, S. (2015). Simulation and prediction of radio frequency heating in dry soybeans. *Biosystems Engineering, 129*, 34–47.

Huang, J. P., Zhang, M., Adhikari, B., & Yang, Z. X. (2016). Effect of microwave air spouted drying arranged in two and three-stages on the drying uniformity and quality of dehydrated carrot cubes. *Journal of Food Engineering, 177*, 80–89.

Huang, Z., Marra, F., Subbiah, J., & Wang, S. (2018). Computer simulation for improving radio frequency (RF) heating uniformity of food products: a review. *Critical Reviews in Food Science and Nutrition, 58*(6), 1033–1057.

Jeong, S. G., Baik, O. D., & Kang, D. H. (2017). Evaluation of radio-frequency heating in controlling Salmonella enterica in raw shelled almonds. *International Journal of Food Microbiology, 254*, 54–61.

Jia, X. R., Zhao, J. Y., & Cai, Y. C. (2015). Radio frequency vacuum drying of timber: mathematical model and numerical analysis. *Bioresources, 10*(3), 5440–5459.

Ju, H. Y., Law, C. L., Fang, X. M., Xiao, H. W., Liu, Y. H., & Gao, Z. J. (2016). Drying kinetics and evolution of the sample's core temperature and moisture distribution of yam slices (*Dioscorea alata* L.) during convective hot-air drying. *Drying Technology, 34*(11), 1297–1306.

Kaya, A., Aydm, O., & Kolayli, S. (2010). Effect of different drying conditions on the vitamin C (ascorbic acid) content of Hayward kiwifruits (*Actinidia deliciosa* Planch). *Food and Bioproducts Processing, 88*(C2–3), 165–173.

Kirmaci, B., & Singh, R. K. (2012). Quality of chicken breast meat cooked in a pilot-scale radio frequency oven. *Innovative Food Science and Emerging Technologies, 14*, 77–84.

Koumoutsakos, A., Avramidis, S., & Hatzikiriakos, S. G. (2001). Radio frequency vacuum drying of wood. II. Experimental model evaluation. *Drying Technology, 19*(1), 85–98.

Li, R., Kou, X., Cheng, T., Zheng, A., & Wang, S. (2017). Verification of radio frequency pasteurization process for in-shell almonds. *Journal of Food Engineering, 192*, 103–110.

Liu, S. X., Ozturk, S., Xu, J., Kong, F. B., Gray, P., Zhu, M. J., Sablani, S. S., & Tang, J. M. (2018). Microbial validation of radio frequency pasteurization of wheat flour by inoculated pack studies. *Journal of Food Engineering, 217*, 68–74.

Marra, F., Zhang, L., & Lyng, J. G. (2009). Radio frequency treatment of foods: review of recent advances. *Journal of Food Engineering, 91*(4), 497–508.

Maskan, M. (2001). Drying, shrinkage and rehydration characteristics of kiwifruits during hot air and microwave drying. *Journal of Food Engineering, 48*(2), 177–182.

Midilli, A., Kucuk, H., & Yapar, Z. (2002). A new model for single-layer drying. *Drying Technology, 20*(7), 1503–1513.

Mrad, N. D., Boudhrioua, N., Kechaou, N., Courtois, F., & Bonazzi, C. (2012). Influence of air drying temperature on kinetics, physico-chemical properties, total phenolic content and ascorbic acid of pears. *Food and Bioproducts Processing, 90*(C3), 433–441.

Mujumdar, A. S. (2007). *Handbook of industrial drying*. Philadelphia: Taylor & Francis.

Orikasa, T., Koide, S., Okamoto, S., Imaizumi, T., Muramatsu, Y., Takeda, J., Shiina, T., & Tagawa, A. (2014). Impacts of hot air and vacuum drying on the quality attributes of kiwifruit slices. *Journal of Food Engineering, 125*, 51–58.

Palazoglu, T. K., & Miran, W. (2018). Experimental investigation of the effect of conveyor movement and sample's vertical position on radio frequency tempering of frozen beef. *Journal of Food Engineering, 219*, 71–80.

Pu, Y. Y., & Sun, D. W. (2016). Prediction of moisture content uniformity of microwave-vacuum dried mangoes as affected by different shapes using NIR hyperspectral imaging. *Innovative Food Science and Emerging Technologies, 33*, 348–356.

Pu, Y. Y., & Sun, D. W. (2017). Combined hot-air and microwave-vacuum drying for improving drying uniformity of mango slices based on hyperspectral imaging visualisation of moisture content distribution. *Biosystems Engineering, 156*, 108–119.

Ramaswamy, H., & Tang, J. (2008). Microwave and radio frequency heating. *Food Science and Technology International, 14*(5), 423–427.

Sagar, V. R., & Kumar, P. S. (2010). Recent advances in drying and dehydration of fruits and vegetables: a review. *Journal of Food Science and Technology, 47*(1), 15–26.

Simal, S., Femenia, A., Garau, M. C., & Rossello, C. (2005). Use of exponential, Page's and diffusional models to simulate the drying kinetics of kiwi fruit. *Journal of Food Engineering, 66*(3), 323–328.

Tavarini, S., Degl'Innocenti, E., Remorini, D., Massai, R., & Guidi, L. (2008). Antioxidant capacity, ascorbic acid, total phenols and carotenoids changes during harvest and after storage of Hayward kiwifruit. *Food Chemistry, 107*(1), 282–288.

Therdthai, N., & Zhou, W. B. (2009). Characterization of microwave vacuum drying and hot air drying of mint leaves (*Mentha cordifolia* Opiz ex Fresen). *Journal of Food Engineering, 91*(3), 482–489.

Tian, Y., Zhang, Y., Zeng, S., Zheng, Y., Chen, F., Guo, Z., Lin, Y., & Zheng, B. (2012). Optimization of microwave vacuum drying of lotus (*Nelumbo nucifera* Gaertn.) seeds by response surface methodology. *Food Science and Technology International, 18*(5), 477–488.

Tiwari, G., Wang, S., Tang, J., & Birla, S. L. (2011). Analysis of radio frequency (RF) power distribution in dry food materials. *Journal of Food Engineering, 104*(4), 548–556.

Uyar, R., Erdogdu, F., & Marra, F. (2014). Effect of load volume on power absorption and temperature evolution during radio-frequency heating of meat cubes: a computational study. *Food and Bioproducts Processing, 92*(3), 243–251.

Vega-Galvez, A., Ah-Hen, K., Chacana, M., Vergara, J., Martinez-Monzo, J., Garcia-Segovia, P., Lemus-Mondaca, R., & Di Scala, K. (2012). Effect of temperature and air velocity on drying kinetics, antioxidant capacity, total phenolic content, colour, texture and microstructure of apple (var. *Granny Smith*) slices. *Food Chemistry, 132*(1), 51–59.

Villa-Corrales, L., Flores-Prieto, J. J., Xaman-Villasenor, J. P., & Garcia-Hernandez, E. (2010). Numerical and experimental analysis of heat and moisture transfer during drying of Ataulfo mango. *Journal of Food Engineering, 98*(2), 198–206.

Wang, S., Birla, S. L., Tang, J., & Hansen, J. D. (2006). Postharvest treatment to control codling moth in fresh apples using water assisted radio frequency heating. *Postharvest Biology and Technology, 40*(1), 89–96.

Wang, Y. C., Zhang, M., Mujumdar, A. S., & Mothibe, K. J. (2013). Microwave-assisted pulse-spouted bed freeze-drying of stem lettuce slices-effect on product quality. *Food and Bioprocess Technology, 6*(12), 3530–3543.

Wang, Y., Zhang, L., Johnson, J., Gao, M., Tang, J., Powers, J. R., & Wang, S. (2014). Developing hot air-assisted radio frequency drying for in-shell macadamia nuts. *Food and Bioprocess Technology, 7*(1), 278–288.

Xiao, H. W., Pang, C. L., Wang, L. H., Bai, J. W., Yang, W. X., & Gao, Z. J. (2010). Drying kinetics and quality of Monukka seedless grapes dried in an air-impingement jet dryer. *Biosystems Engineering, 105*(2), 233–240.

Zhang, M., Tang, J., Mujumdar, A. S., & Wang, S. (2006). Trends in microwave-related drying of fruits and vegetables. *Trends in Food Science and Technology, 17*(10), 524–534.

Zhang, M., Chen, H. Z., Mujumdar, A. S., Tang, J. M., Miao, S., & Wang, Y. C. (2017). Recent developments in high-quality drying of vegetables, fruits, and aquatic products. *Critical Reviews in Food Science and Nutrition, 57*(6), 1239–1255.

Zheng, A., Zhang, L., & Wang, S. (2017). Verification of radio frequency pasteurization treatment for controlling *Aspergillus parasitius* on corns. *International Journal of Food Microbiology, 249C*, 27–34.

Zhou, L. Y., Ling, B., Zheng, A. J., Zhang, B., & Wang, S. J. (2015). Developing radio frequency technology for postharvest insect control in milled rice. *Journal of Stored Products Research, 62*, 22–31.

Zhou, X., Gao, H., Mitcham, E. J., & Wang, S. (2018a). Comparative analyses of three dehydration methods on drying characteristics and oil quality of in-shell walnuts. *Drying Technology, 36*(4), 477–490.

Zhou, X., Li, R., Lyng, J. G., Wang, S. (2018b). Dielectric properties of kiwifruit associated with a combined radio frequency vacuum and osmotic drying. *Journal of Food Engineering, 239*, 72–82.

Zhou, X., & Wang, S. (2018). Recent developments in radio frequency drying of food and agricultural products: a review. *Drying Technology, 36*(16), 2030–2045. https://doi.org/10.1080/07373937.2018.1452255.

Zielinska, M., & Michalska, A. (2016). Microwave-assisted drying of blueberry (*Vaccinium corymbosum* L.) fruits: drying kinetics, polyphenols, anthocyanins, antioxidant capacity, colour and texture. *Food Chemistry, 212*, 671–680.

Zielinska, M., Sadowski, P., & Blaszczak, W. (2015). Freezing/thawing and microwave-assisted drying of blueberries (*Vaccinium corymbosum* L.). *LWT- Food Science and Technology, 62*(1), 555–563.